



# The impact of Neurofeedback on effective connectivity networks in chronic stroke patients: an exploratory study

Giulia Lioi, Adolfo Veliz, Julie Coloigner, Quentin Duché, Simon Butet, Mathis Fleury, Emilie Leveque-Le Bars, Elise Bannier, Anatole Lécuyer, Christian Barillot, et al.

## ► To cite this version:

Giulia Lioi, Adolfo Veliz, Julie Coloigner, Quentin Duché, Simon Butet, et al.. The impact of Neurofeedback on effective connectivity networks in chronic stroke patients: an exploratory study. *Journal of Neural Engineering*, 2021, 18 (5), pp.056052. 10.1088/1741-2552/ac291e . hal-03354296

**HAL Id: hal-03354296**

**<https://imt-atlantique.hal.science/hal-03354296>**

Submitted on 19 Nov 2021

**HAL** is a multi-disciplinary open access archive for the deposit and dissemination of scientific research documents, whether they are published or not. The documents may come from teaching and research institutions in France or abroad, or from public or private research centers.

L'archive ouverte pluridisciplinaire **HAL**, est destinée au dépôt et à la diffusion de documents scientifiques de niveau recherche, publiés ou non, émanant des établissements d'enseignement et de recherche français ou étrangers, des laboratoires publics ou privés.

## Title

**The Impact of Neurofeedback on Effective Connectivity Networks in Chronic Stroke Patients: an exploratory study**

## Authors

**Lioi Giulia<sup>1,4\*§</sup>, Veliz Adolfo<sup>1§</sup>, Coloigner Julie<sup>1</sup>, Duché Quentin<sup>1,2</sup>, Butet Simon<sup>2</sup>, Mathis Fleury<sup>1</sup>, Emilie Leveque-Le Bars<sup>2</sup>, Elise Bannier<sup>1,3</sup>, Anatole Lécuyer<sup>1</sup>, Christian Barillot<sup>1†</sup>, Isabelle Bonan<sup>2†</sup>**

1 Univ Rennes, Inria, CNRS, Inserm, IRISA, Rennes, France

2 CHU Rennes, Departement of Physical and Rehabilitation Medicine, Rennes, France

3 CHU Rennes, Departement of Radiology, Rennes, France

4 IMT Atlantique, Lab-STICC, UMR CNRS 6285, F-29238, France

\*corresponding author [giulia.lioi@imt-atlantique.fr](mailto:giulia.lioi@imt-atlantique.fr)

§These authors have contributed equally to the work

† These authors have contributed equally to the work

## Keywords

**Neurofeedback, Effective Connectivity, Stroke Rehabilitation, Dynamic Causal Modeling, fMRI**

## Abstract

### Objective

In this study, we assessed the impact of EEG-fMRI Neurofeedback (NF) training on connectivity strength and direction in bilateral motor cortices in chronic stroke patients. Most of the studies using NF or brain computer interfaces for stroke rehabilitation have assessed treatment effects focusing on successful activation of targeted cortical regions. However, given the crucial role of brain network reorganization for stroke recovery, our broader aim was to assess connectivity changes after a NF training protocol targeting localised motor areas.

### Approach

We considered changes in fMRI connectivity after a multisession EEG-fMRI NF training targeting ipsilesional motor areas in nine stroke patients. We applied the Dynamic Causal Modeling and Parametric Empirical Bayes frameworks for the estimation of effective connectivity changes. We considered a motor network including both ipsilesional and contralesional premotor, supplementary and primary motor areas.

### Main results

Our results indicate that NF upregulation of targeted areas (ipsilesional supplementary and primary motor areas) not only modulated activation patterns, but also had a more widespread impact on fMRI bilateral motor networks. In particular, inter-hemispheric connectivity between premotor and primary motor regions decreased, and ipsilesional self-inhibitory connections were reduced in strength, indicating an increase in activation during the NF motor task.

Significance

To the best of our knowledge, this is the first work that investigates fMRI connectivity changes elicited by training of localized motor targets in stroke. Our results open new perspectives in the understanding of large-scale effects of NF training and the design of more effective NF strategies, based on the pathophysiology underlying stroke-induced deficits.

## Introduction

A growing body of evidence suggests that post-stroke motor deficits are related to altered interactions between brain areas also remote from the stroke lesion [1]. Indeed, localized structural lesions resulting from stroke are likely to affect brain connectivity through the brain. As a consequence, recovery from stroke depends on structural and functional networks reorganization [2]–[5]. These findings are in line with the increasingly influential thesis that most of complex biological diseases, such as motor disorders [1], psychiatric disorders [6] or Alzheimer disease [7] are related to the dysfunction of complex brain networks [8].

In stroke in particular, several studies have used brain functional neuroimaging techniques such as positron emission tomography (PET), functional Magnetic Resonance imaging (fMRI) and electroencephalography (EEG) to investigate changes in brain activity [9], [10]. More recently, connectivity-based analyses have shed new light into the pathophysiology underlying stroke-induced deficits [4], [11], [12]. A general trend observed in these studies is that stroke induces changes in both hemispheres and causes a disruption of ipsilesional connectivity [13]. Some of these connectivity-based approaches have gone further and investigated the effect of interventions (such as physical or robotic assisted therapy) on cortical network reorganization, and its link to motor function recovery [14]. However, the impact of specific therapies on motor connectivity in stroke remains to be investigated. Assessment of changes in connectivity networks induced by treatment is now considered to be a promising way to individualize therapies and enhance rehabilitation outcome after stroke [1].

There are different ways of estimating brain connectivity from neuroimaging data. Structural connectivity refers to anatomical connections between brain regions and is most commonly estimated using Diffusion Tensor Imaging (DTI). Functional connectivity (FC) is defined as the statistical dependence among measurements of neural activity [15] and it is usually inferred through correlations among neurophysiological signals. Effective connectivity (EC) estimates the influence that one neuronal system exerts on another. EC is intrinsically directed, but does not necessarily imply a direct coupling mediated by anatomical connections. Connectivity studies in stroke have relied both on FC [16], [17] and EC [3], [18], [19]. Among EC estimators, those based on Dynamic Causal Modeling (DCM) are particularly robust for fMRI data analysis, while lag-based approach (i.e. Granger causality) may perform poorly if the hemodynamic effects are not properly taken in account [20].

Among the set of therapies proposed for stroke rehabilitation, Neurofeedback (NF) is gaining increasing attention since it potentially promotes plasticity of perilesional areas by means of brain self-regulation. Recent works have investigated the potential of NF (or Brain Computer Interfaces, BCI) for motor rehabilitation after stroke as an alternative or in addition to traditional physical therapies [21]–[25]. In these studies, patients perform motor imagery (MI) of the affected limb, which is a promising mental therapy to restore motor activation. Even if there is no clinical evidence of the benefit of NF over MI for

stroke rehabilitation, NF was shown to enhance the efficacy of MI training, by eliciting more specific brain patterns [26], [27]. In some applications, the NF paradigm allows to integrate the feedback in an orthosis to support the movement of the affected limb, thus closing the sensorimotor loop [28], [29].

The majority of these NF approaches have relied on one imaging technique, mainly electroencephalographic (EEG) recordings. EEG-NF applications are generally based on the training of sensorimotor rhythms in motor regions ipsilateral to the stroke lesion [30]–[32]. Similarly, more recent fMRI-NF studies have promoted upregulation of ipsilesional motor areas or motor system connectivity [23], [33]–[35]. Building on the pioneering work of Zotev and collaborators [36], [37], we integrated EEG and fMRI for bimodal NF for motor training, with the rationale of providing a more specific feedback, combining high temporal (EEG) and spatial (fMRI) resolution [38]. We have also shown the feasibility of EEG-fMRI NF and its potential to promote upregulation of ipsilesional motor regions in a pilot study involving chronic stroke patients [24]. In this previous work, we have investigated NF training effects focusing on the activation of localized target cortical areas. In the present study, we characterize global changes elicited by NF training on EC networks in chronic stroke patients undergoing a longer NF training protocol. We assessed fMRI connectivity changes using a DCM approach and considered a motor network including bilateral premotor, supplementary and primary motor areas (PMC, SMA, M1). We believe that our results bring new insight into large-scale effects of NF training in stroke and on the potential of NF in driving maladaptive networks reorganization.

## **Methods**

### *Participants*

Nine chronic stroke patients (mean age 59 years, age range: 37-77 years, 3 females) were included in the study. Patients had mild to severe hemiparesis of the upper limb (Upper extremity Fugl-Meyer score in the range 26-55) with variable lesion characteristics (Table 1) but were clinically stable, at more than one year from the stroke episode ( $33.2 \pm 16.5$  months). Integrity of the corticospinal tract (CST) was an inclusion criterion. Patients for whom the CST fractional anisotropy asymmetry index exceeded the 0.15 threshold [39] were not enrolled. More details about diffusion imaging processing and CST segmentation are given in Supplementary Material. This study is part of a larger randomized controlled study to assess the efficacy of NF (NCT03766113). In this exploratory work, we considered a subsample of participants with the aim of validating data quality and investigating the effect of NF training on motor connectivity. All participants gave their written informed consent and the study was approved by the institutional review board and registered.

### *Experimental Protocol*

Participants underwent a NF protocol alternating bimodal EEG-fMRI NF (N=5) and unimodal EEG-NF sessions (N=9) over a period of five weeks. NF sessions included a calibration and three NF training blocks alternating epochs of rest (20 s) and NF-MI training (20 s) (Figure S1). Patients were informed at inclusion, verbally and by an explanatory note, about the goals and the timeline of the study. Instructions were repeated before each training session and oriented the patients towards a kinesthetic MI of the affected upper limb, without mentioning a specific strategy.

Imaging was performed using a Siemens 3T Prisma scanner running VE11C and a 64-channel MR-compatible EEG system from Brain Products (Brain Products GmbH, Gilching, Germany). Functional MRI data were acquired with echo-planar imaging (EPI) with the following parameters: repetition time

(TR)/echo time (TE) = 1,000/23 ms, FOV =  $230 \times 230 \text{ mm}^2$ , 16 4-mm slices, voxel size =  $2.2 \times 2.2 \times 4 \text{ mm}^3$ , matrix size =  $105 \times 105$ , flip angle =  $90^\circ$ . For each session, a high-resolution 3D T1 MPRAGE sequence was acquired with the following parameters: TR/TI/TE = 1,900/900/2.26 ms, parallel imaging with GRAPPA 2, FOV =  $256 \times 256 \text{ mm}^2$  and 176 slabs, voxel size =  $1 \times 1 \times 1 \text{ mm}^3$ , flip angle =  $9^\circ$ . In order to assess the asymmetry between the ipsilesional and contralesional CST, diffusion imaging (TR/TE=11000/99ms, FOV  $256 \times 256 \text{ mm}^2$ , 60 slices, matrix  $128 \times 128$ , voxel size,  $2 \times 2 \times 2 \text{ mm}^3$ , 30 directions,  $b=1000 \text{ s/mm}^2$ ) was performed before inclusion. During rest, a cross was displayed on the screen and participants were asked to concentrate on the cross and rest. During the task, a visual feedback in the form of a ball moving in a one-dimensional gauge proportionally to the average of the EEG and the fMRI features was presented. More specifically, the bimodal NF was calculated as the normalized average of the EEG- NF score (Event Related Desynchronization in the 8-30 Hz band of 18 motor electrodes, updated every 250 ms) and fMRI NF score (weighted sum of the difference between percentage signal change in the two ROIs (SMA and M1) and a large deep background region, updated every TR=1 s), as explained in more detail in the supplementary material. Unimodal EEG-NF sessions were performed using the Mensia Modulo (MENSIA TECHNOLOGIES) hardware solution, equipped with an 8-channel EEG cap. Patients were exposed to the same feedback metaphor on a computer screen. More details about the NF platform performing real-time EEG-fMRI processing, the unimodal NF sessions and the experimental protocol are given in [24], [38], [40] and in the attached Supplementary Material.

#### *Calibration and online NF calculation*

At the beginning of each training session, a MI task without NF was performed to calibrate the fMRI signal. Functional MRI data were pre-processed for motion correction and slice-time correction and realigned with the structural scan. After spatial smoothing with a 6 mm FWHM Gaussian kernel, a general linear model (GLM) analysis was performed. The calibration activation map was used to define two regions of interest (ROIs) to calculate NF scores for the subsequent NF task. Boxes of  $9 \times 9 \times 3$  voxels ( $20 \times 20 \times 12 \text{ mm}^3$ ) centered on the peak of activation in the ipsilesional SMA and M1 were considered. As detailed in a previous work [24], we proposed an adaptive rewarding strategy that more importantly weighted SMA at the beginning of the training and then guided the patients towards activation of the ipsilesional M1. The rationale behind this adaptive NF training is that ipsilesional M1 is considered the ideal target for motor recovery. However, while SMA seems to be more robustly and easily recruited during MI, M1 activation during MI is more difficult to achieve [41], [42]. The proposed NF reinforcement scheme aims at gradually guiding the patients towards the activation of the ipsilesional primary motor cortex, while first engaging more importantly the supplementary motor areas. The fMRI NF score was therefore calculated as a weighted combination of the activity in the SMA and M1 ROIs, with weights changing at each training session. In particular the fMRI-NF score was calculated as the difference between percent signal change in the two ROIs (SMA and M1) and a background slice whose activity is not correlated with the NF task, in order to reduce the impact of global signal changes [43].

For the sake of brevity of this manuscript focusing on fMRI effective connectivity analysis, we have provided more details about calibration and NF calculation procedure in Supplementary Material. A CRED-nf checklist with details about experimental design [44] is also available as Supplementary File 1 together with a table summarizing real-time signal processing steps, according to the COBIDAS-inspired template [45] (Table S1, Supplementary Material).

#### *fMRI preprocessing*

164 In order to assess the effect of the multi-session NF training protocol on EC patterns, we considered  
 165 fMRI time-series of the first (b-s1) and last (b-s5) bimodal NF training sessions. BOLD series were pre-  
 166 processed and processed with Matlab and SPM12 (Wellcome Department of Imaging Neuroscience,  
 167 UCL, London, UK). A slice timing correction was applied to correct for timing differences within volumes.  
 168 Functional volumes were then registered to the mean volume to compensate for subject motion within  
 169 the series and ensure voxel-to-voxel correspondence across time. The mean fMRI image was co-  
 170 registered with the subject structural image. The anatomical volume was in turn segmented and non-  
 171 linearly transformed to the reference Montreal Neurological Institute (MNI) space. The estimated  
 172 normalization deformations fields were later applied to functional data that were finally smoothed using  
 173 a 3D Gaussian kernel of 6 mm FWHM.

174 An offline data quality control was performed to assess for the impact of head movement artifacts on  
 175 data quality and NF performances. Motion parameters were estimated and used to perform a post-hoc  
 176 correlation analysis with the NF task. To this end and for each bimodal session a Framewise  
 177 Displacement (FD) was computed from the six realignment parameters as proposed by Power et al. [46].  
 178 FD outliers were identified using the spmup tool within the QAP Package [47]. Pearson correlation  
 179 analysis between the FD time-series and the NF task was assessed.

180 At the subject level, each session was modeled using a three-run generalized linear model (GLM), where  
 181 each NF block and each rest block were modeled by convoluting a 20s boxcar function with the standard  
 182 hemodynamic response function (HRF) to build a NF task and a rest regressors. The estimated motion  
 183 parameters and a run mean were also entered in the design matrix as covariates of no interest. NF  
 184 blocks and rest blocks were contrasted run-wise in order to analyze the NF effect session-wise but also  
 185 averaged over the three runs to evaluate the NF effect over the whole bimodal session. The normalised  
 186 individual contrast maps of the three patients with right lesions were flipped along the y axis to create  
 187 an artificial group of 9 patients with left-only hemispheric lesions. These maps were entered into a  
 188 training session specific second level analysis GLM to evaluate group activation maps at each NF training  
 189 session, allowing to monitor the effect of NF on brain activation.

190 The evolution of the NF effect over bimodal sessions was evaluated within a two-step procedure at both  
 191 the individual and group level. At the individual level, individual NF-rest contrast maps were entered in  
 192 the design matrix. At the group level, NF-rest group contrast maps obtained from the previous GLM  
 193 analysis were entered in the design matrix. In both cases, 14 session-wise NF-rest contrast maps were  
 194 entered in the first column of the linear increase design matrix. A time regressor ranging from 1 to 14  
 195 coding for the NF session index was added as a second column. By contrasting the effect of time,  
 196 resulting statistical maps provided voxels or clusters demonstrating a linear increase (or decrease) of  
 197 (group or individual) brain activity over the NF sessions.

#### 198 *ROI definition and time series extraction*

199 In order to discard task independent noise, representative time series for the selected ROIs were  
 200 extracted by considering the voxels which, in the first level GLM analysis, exceeded the statistical  
 201 threshold for NF contrast ( $p < 0.01$ ), and were located within an apriori mask for bilateral SMA, PMC and  
 202 M1. These masks were defined using the Human Motor Area Template (HMAT) atlas [48]. The SMA  
 203 mask included both preSMA and SMA HMAT ROIs, and the PMC included ventral and dorsal PMC. To  
 204 adapt the selected ROIs to individual responses, we extracted the first principal component of the time  
 205 series from all voxels within 8-mm spheres around local activation maxima [49]. As for whole brain

analysis, ROIs time series were flipped in the case of patients with a right hemisphere lesion (N=3) for the sake of the group analysis (in the group results of the affected hemisphere is thus presented on the left).

#### *Dynamical causal modeling (DCM)*

DCM is a hypothesis-based technique that describes how observed fMRI responses are generated using a set of differential equations and represents one of the most common frameworks for the analysis of fMRI effective connectivity [50]. These differential equations describe how experimental stimulation (input) produces changes in neural activity and induces changes in the output (i.e. the observed fMRI data) through a hemodynamic model [51]. DCM models include parameters, such as the strength of coupling between the ROIs, i.e. effective connectivity, which are estimated from the data using a variational Laplace approach [52].

In the current DCM study, we assessed the differences in DCM parameters between the first (b-s1) and last (b-s5) NF session and considered a model consisting of six motor regions with bidirectional connections among them all (PMCL, PMCR, SMA<sub>L</sub>, SMA<sub>R</sub>, M1<sub>L</sub>, and M1<sub>R</sub>). These regions were selected on the basis of the evidence of their role in MI and previous connectivity stroke studies [4], [14], [53]. In this study we focused on endogenous connectivity analysis (DCM matrix A) [49] and assessed how its strength is modulated by the NF training.

In the first step of the analysis, a Bayesian model selection procedure for each subject was performed to estimate the model that best matched the measured fMRI data. The basic 6 ROIs model was elaborated into 10 more different models depending upon which premotor region (SMA and PMC) was modulated by the external experimental input (NF task) and a 'null' model with no modulation. The different models (represented in Figure S6 in Supplementary Material) were compared and an optimal DCM model for each subject and session was identified using the Bayesian model selection.

After all DCM models were estimated and every subject connectivity strengths was inferred, we performed a group level analysis to assess differences and commonalities between patients using the recently introduced Parametrical Empirical Bayes (PEB) approach [54]. To test hypotheses about between-subjects effects, individual differences in coupling parameters are decomposed into hypothesized group level effects, called regressors or covariates, and unexplained variance or random effects. Since the aim of this study was to assess the effect of the NF training on the EC strength, we introduce this covariate of interest in the PEB analysis. In order to exclude other factors independent from the training, the Fugl-Meyer score, FA asymmetry index, type of stroke and time from stroke were also included as regressors in the between-subjects analysis. We applied PEB to each model and extracted the free energy, which is an approximation of the log-evidence of the model that considers both accuracy and complexity [52], compared them and selected a winning model. The winning model was then considered for the posterior analysis and the group level results. Note that while in first level analysis individual connectivity models are estimated for each patient, the group level PEB analysis assumes a unique model for all the subjects. The estimation of a unique "winning" model enables us to test hypotheses about the common experimental effects on the connectivity strength of the population.

Finally, after having identified the winning model, an automatic search over reduced models was performed by means of Bayesian Model Reduction (BMR) [54]. To summarize the results over all the models, a Bayesian Model Average (BMA) was computed [55] by averaging the parameters from

different reduced models, weighted by the model posterior probabilities. When showing summary BMA results, we only considered parameters with a strong evidence (i.e. posterior probability of being non-zero greater than 0.99). All the computations were performed using the DCM analysis code adapted from SPM12, described step-by-step in [49], [56] and available at <https://github.com/pzeidman/dcm-peb-example>. Other scripts used for fMRI and DCM analysis in this paper can be provided by the authors upon request. More details about code availability are also given in Supplementary Material.

## Results

Despite the demanding and intensive training protocol, no drops-out were registered: participants found the training satisfying and completed it.

### *fMRI activation analysis*

Even if a thorough analysis of changes in BOLD activation patterns is outside the main scope of this work, which focuses on effective connectivity changes after NF training, we summarize in this paragraph main results. More details about fMRI analysis and additional results are provided in the Supplementary Material.

The motion artifacts analysis revealed that in 5 out of 45 training sessions the percentage of head motion outliers was higher than 10%. Also, in 11% of sessions (6 out of 45) the Pearson correlation between the head motion and the NF task regressor was higher than 0.25 (in absolute value). These findings are similar to those reported in a previous study on 30 healthy volunteers [57]. Additional details and results of the offline data quality check are given in Supplementary Material (Table S1 and Figures S1 and S2).

Figure 1 presents group activation maps ( $N=9$ ) in the first (b-s1) and last (b-s5) NF training session, that were then considered for DCM analysis. Reported statistical maps show activations exceeding a voxel-level uncorrected threshold of  $p<0.001$ . Average BOLD activation maps show significant activations of the premotor cortex and supplementary motor areas. The bilateral posterior parietal cortex (PPC), that plays an important role in visuo-motor coordination [58], was also recruited during the MI NF task. In general, patients robustly activated mainly the bilateral SMA during the first session (b-s1), while they showed also activation of the bilateral PMC and ipsilesional M1 in the last NF session (b-s5).

Together with differences between the first and last NF session, we also investigated if there was a significant linear increase of BOLD activation across the 14 NF runs of the five bimodal sessions. Group results in Figure 2 suggest that bilateral SMA and PMC BOLD activation linearly increased from one session to another (clusters of  $k>25$  voxels,  $p<0.001$ , uncorrected). A localized increase could be observed also in the ipsilesional M1, but did not correspond to an increase in the contralesional M1. Individual maps indicate that activation patterns across patients are variable, even if a linear increase in activation of SMA and PMC can be observed in the majority of the individuals (Figure S4a). Similarly, the analysis of offline NF scores for SMA and M1 indicated that a significant increase in the average SMA NF score was observed in the majority of patients, while results concerning M1 NF scores are more variable across individuals (Figure S4a and S4b).



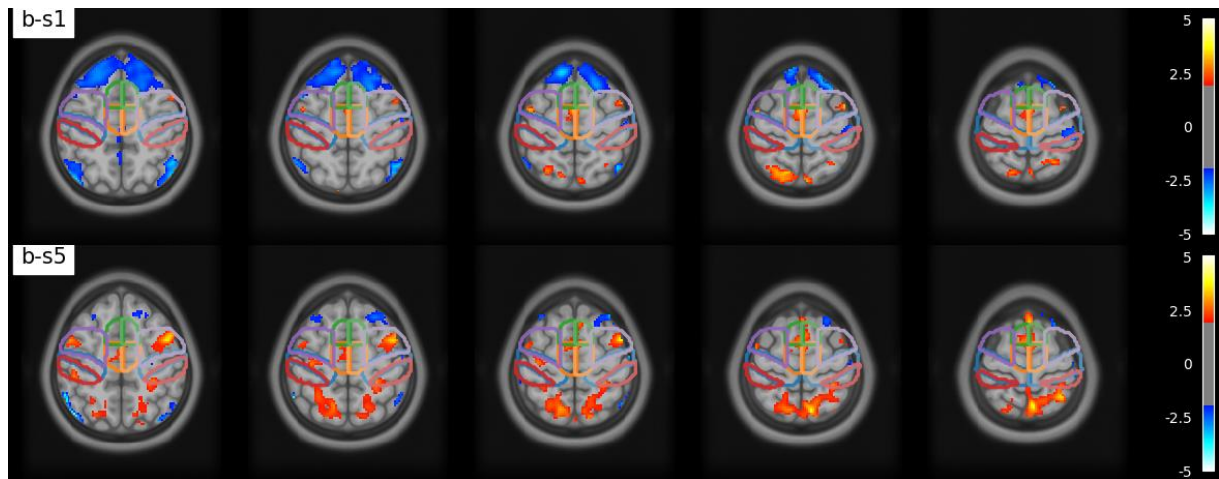


Figure 1. Group activation maps in the first (b-s1) and last (b-s5) training session in MNI coordinates ( $p < 0.05$ , uncorrected). The outline of the motor areas of interest based on the HMAT atlas is indicated: preSMA (green) SMA (orange), PMC (purple), M1 (blue) and Sensory motor cortex (red). The lesional hemisphere is on the left (results for the patients whose lesion was in the right hemisphere were flipped for the sake of comparison).

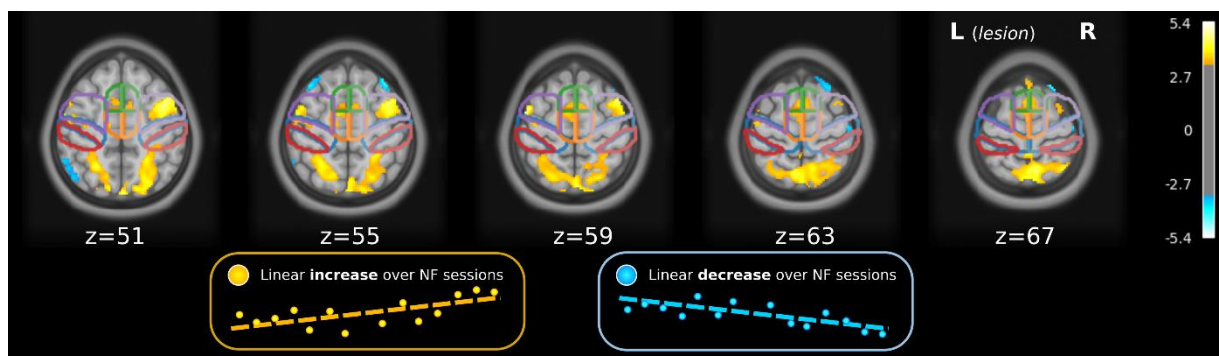


Figure 2. BOLD activation linear increase along NF sessions. Cluster of voxels ( $k > 25$ ) exhibiting a significant linear increase (decrease) over the 14 bimodal NF runs are showed in yellow (light blue) ( $p < 0.001$ , uncorrected). The outline of the motor areas of interest based on the HMAT atlas is indicated: preSMA (green) SMA (orange), PMC (purple), M1 (blue) and Sensory motor cortex (red). The lesional hemisphere is on the left (results for the patients whose lesion was in the right hemisphere were flipped for the sake of comparison).

#### DCM analysis: changes in endogenous connectivity

The subject average percentage variance explained by the model is 10.5% (SD 7.3%): it compares to other results in literature [49] but is smaller. This is to be expected in the case of simultaneous EEG-fMRI imaging considered the decrease in fMRI signal to noise ratio due to the presence of EEG electrodes [59]. In most of the subjects, coupling parameters were non-trivial, with 90% credible intervals that excluded zero, indicating that there was useful information in the data pertaining to the NF experimental effects. The PEB free energy, considered to be a proxy for the log model evidence, was of  $-1.012 \times 10^5$  (a graph reporting the free energy corresponding to the 10 DCM models is reported in Supplementary Material, Figure S7).

Endogenous connectivity patterns elicited during MI NF obtained from the BMA analysis are schematically represented in Figure 3 and the corresponding values are listed in Table 2. Coupling

parameters in average connectivity patterns (i.e. common to all subjects and sessions) quantify the EC from one area over another in Hz. Negative coupling rates indicate that the source region has an inhibitory effect on the activity of the target region (in red in Figure 3), while positive EC values indicate an excitatory effect (in green in Figure 3). Inhibitory self-connections scale up or down the default value of 0.5 Hz [49] therefore positive self-connection values indicate increased self-inhibition while negative values indicate activation of the specific region. As shown in Figure 3A, experimental driving inputs (NF MI task) had a positive influence on bilateral premotor areas: this is consistent with the recruitment of PMC during a MI task [60]. The average EC results indicate a fully connected motor network, with mainly excitatory coupling, involving both hemispheres. Connectivity between contralesional and ipsilesional motor areas was also elicited during the MI task of the affected limb. Self-connection values were negative for all ROIs, indicating a significant disinhibition, or equivalently an activation, of all the considered motor regions during the NF MI task.

In Figures 3B and 4 modulatory effects of the NF training on EC strength are represented, with positive connections (green) indicating an average increase in connectivity between ROIs and negative connections (red) representing a decrease in EC between the first and last NF training session. A general trend of decrease in inter-hemispheric connectivity strength can be observed, in particular between contralesional (right) and ipsilesional (left) PMC and M1. Only connections originating from SMA towards the M1 and PMC increased in strength following the NF training, while feedback connectivity from ipsilesional M1 to all other motor areas was reduced (except for the connection to ipsilesional PMC that increased). A decrease in self-inhibition strength in bilateral SMA and ipsilesional M1 was observed: this indicates a higher activation of these regions as a result of training, in line with the results of the whole brain analysis presented in Figures 1 and 2. In order to assess the variability in connectivity strength changes across subjects, we calculated the difference between individual endogenous connectivity (matrices A) in b-s1 and b-s5. Representative results for six connections (ipsilesional, contralesional and intrahemispheric EC) are shown in Figure 4 and indicate consistent findings: individual connectivity strength have the same signs and similar amplitudes across patients. Additional results can be found in Figures S5 and S6.

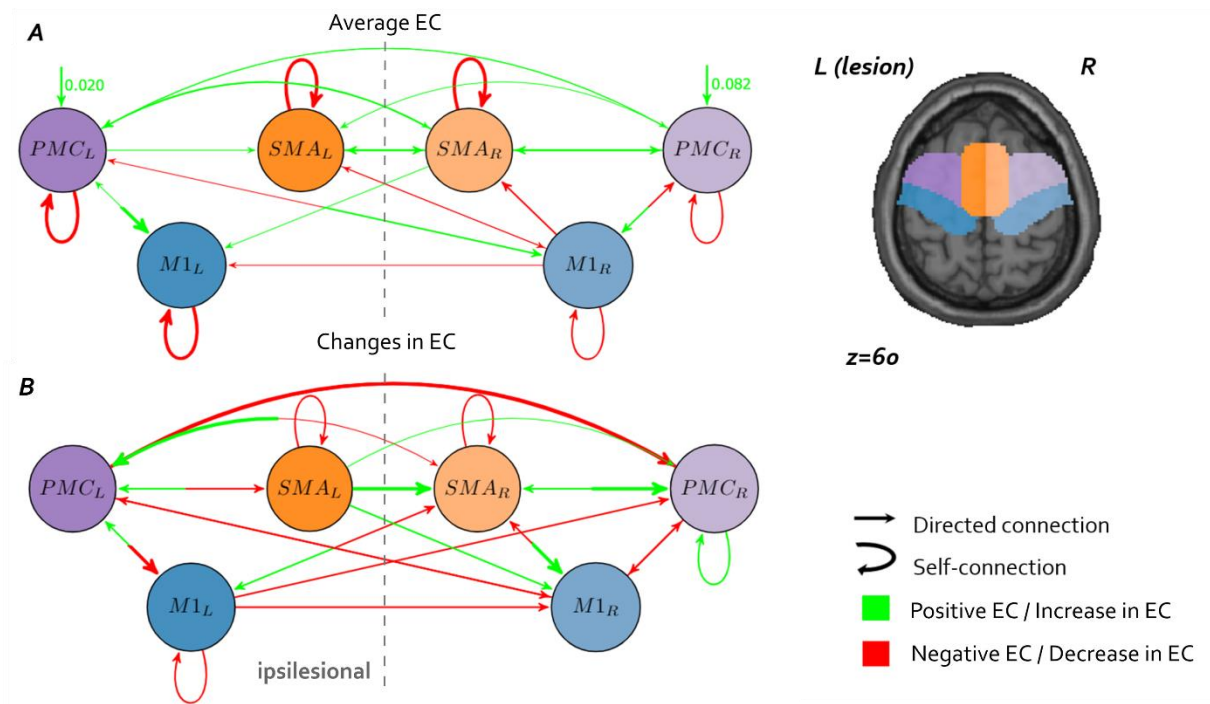


Figure 3. Bayesian Model Average (BMA) results. A. Connectivity network commonalities across subjects and training sessions. Arrows thickness and color code respectively for the strength and the sign of EC: green arrows represent a positive (excitatory) coupling, while red arrows indicate negative coupling. B. Significant changes ( $p < 0.01$ ) in EC strength after the NF training. Arrows thickness and color code respectively for the strength and the sign of EC change: green arrows represent an increase in connectivity, while red arrows indicate a decrease. The direction of links is represented by the arrow's ending. Since EC is not symmetrical, an opposite change in connectivity can be observed between two regions. It is the case of regions connected by a "bicolor" arrow (i.e. in panel B the arrow between  $M1_L$  and  $PMC_L$  indicate an increase of the connectivity from  $M1_L$  to  $PMC_L$  and a decrease of connectivity from  $PMC_L$  to  $M1_L$ ).

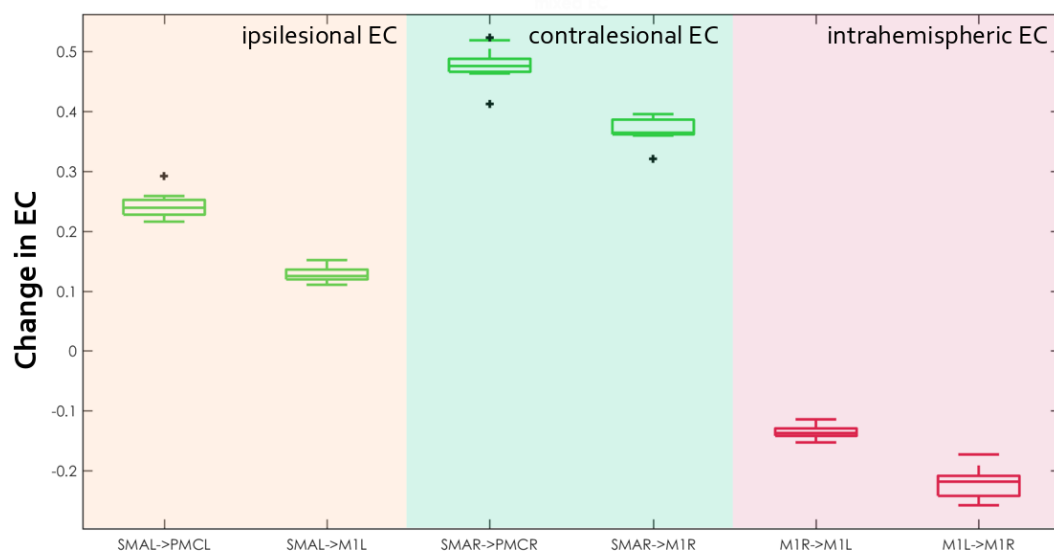


Figure 4. Changes in EC connectivity across patients for six representative connections. Boxplots indicate the median (central mark) and the 25th and 75th percentiles (bottom and top edges of the box) of the EC changes across 9 patients. Outliers are shown with a black cross. Green boxplots correspond to an increase in connectivity strength from b-s1 to b-s5; inversely red boxplots correspond to a decrease in EC after NF training.

350 *Table 1. Patients demographic and stroke characteristics.*

Patient ID	Gender	Time from stroke (months)	Stroke type	Stroke lesion	Fugl-Meyer	FA_asymmetry
P01	F	25	Ischemic, middle left cerebral artery	Left	53	0.0257
P02	M	34	Ischemic, middle left cerebral artery	Left	50	0.0180
P03	M	68	Subcortical haemorrhagic stroke	Right	26	0.12
P04	M	49	Ischemic, middle left cerebral artery	Left	29	0.0590
P05	M	28	Ischemic, middle left cerebral artery	Left	39	0.002
P06	M	199	Left haemorrhagic	Left	26	0.124
P07	M	36	Ischemic, middle left cerebral artery	Left	42	-0.008
P08	F	26	Ischemic, middle right cerebral artery	Right	55	0.001
P09	F	14	Ischemic, middle right cerebral artery	Right	52	0.098

351

*Table 2. Bayesian Model Average of PEB parameters: Average endogenous connectivity and significant changes in connectivity strength as a result of the NF training.*

Source	Target	Commonalities	Effect of Treatment
SMA <sub>L</sub>	SMA <sub>L</sub>	-0.3616	-0.1339
SMA <sub>L</sub>	PMC <sub>L</sub>	-0.0000	0.0893
SMA <sub>L</sub>	M1 <sub>L</sub>	-0.0000	0.0000
SMA <sub>L</sub>	SMA <sub>R</sub>	0.2396	0.1784
SMA <sub>L</sub>	PMC <sub>R</sub>	0.0000	0.0856
SMA <sub>L</sub>	M1 <sub>R</sub>	-0.0902	0.1140
PMC <sub>L</sub>	SMA <sub>L</sub>	0.1077	-0.1608
PMC <sub>L</sub>	PMC <sub>L</sub>	-0.4562	0.0000
PMC <sub>L</sub>	M1 <sub>L</sub>	0.3510	-0.2343
PMC <sub>L</sub>	SMA <sub>R</sub>	0.0904	-0.0808
PMC <sub>L</sub>	PMC <sub>R</sub>	0.1367	-0.1872
PMC <sub>L</sub>	M1 <sub>R</sub>	0.2282	-0.1034
M1 <sub>L</sub>	SMA <sub>L</sub>	0.0000	0.0000
M1 <sub>L</sub>	PMC <sub>L</sub>	0.0860	0.0890
M1 <sub>L</sub>	M1 <sub>L</sub>	-0.3818	-0.1635
M1 <sub>L</sub>	SMA <sub>R</sub>	0.0000	-0.1213
M1 <sub>L</sub>	PMC <sub>R</sub>	0.0000	-0.0995
M1 <sub>L</sub>	M1 <sub>R</sub>	0.0000	-0.0974
SMA <sub>R</sub>	SMA <sub>L</sub>	0.1752	0.0460
SMA <sub>R</sub>	PMC <sub>L</sub>	0.2006	0.1830
SMA <sub>R</sub>	M1 <sub>L</sub>	0.0830	0.1711
SMA <sub>R</sub>	SMA <sub>R</sub>	-0.3444	-0.1195
SMA <sub>R</sub>	PMC <sub>R</sub>	0.2365	0.2620
SMA <sub>R</sub>	M1 <sub>R</sub>	0.0000	0.1753
PMC <sub>R</sub>	SMA <sub>L</sub>	0.1227	0.0000
PMC <sub>R</sub>	PMC <sub>L</sub>	0.0818	-0.1786
PMC <sub>R</sub>	M1 <sub>L</sub>	0.0000	-0.0000
PMC <sub>R</sub>	SMA <sub>R</sub>	0.2782	0.0876
PMC <sub>R</sub>	PMC <sub>R</sub>	-0.2467	0.1195
PMC <sub>R</sub>	M1 <sub>R</sub>	0.2232	-0.1084
M1 <sub>R</sub>	SMA <sub>L</sub>	-0.0972	-0.0000
M1 <sub>R</sub>	PMC <sub>L</sub>	-0.1026	-0.1469
M1 <sub>R</sub>	M1 <sub>L</sub>	-0.0783	0.0000
M1 <sub>R</sub>	SMA <sub>R</sub>	-0.2783	-0.1223
M1 <sub>R</sub>	PMC <sub>R</sub>	-0.1689	-0.1324
M1 <sub>R</sub>	M1 <sub>R</sub>	-0.2707	0.0000

## Discussion

We applied a DCM analysis to task-based fMRI data to describe the effect of NF training on bilateral motor networks in nine chronic stroke patients. The training protocol included five bimodal EEG-fMRI NF and nine EEG-NF sessions over five weeks aiming at reinforcing the activity of specific motor areas (ipsilesional SMA and M1). Results indicate that NF training induced a modulation of fMRI activation during the NF MI task towards ipsilesional motor cortex activation. We also found a reorganization of

effective connectivity after training, with a general trend to reduced inter-hemispheric connectivity between premotor and primary motor cortices. These exploratory results suggest that the training of specific motor areas with NF can have an impact overall motor connectivity network.

## *Methods*

Different estimators of EC from fMRI data are available [61]. In this study, we used DCM for EC estimation because it was specifically developed for fMRI analysis. DCM has the advantage over approaches such as structural equation modeling or Granger causality that it uses a hemodynamic model to decompose the measured data into underlying neuronal signal and hemodynamic effects [50]. Moreover, DCM is particularly robust in dealing with deviations from the standard hemodynamic response (*e.g.* due to pathology affecting blood flow parameters such as stroke), as the parameters in the hemodynamic model are estimated together with the parameters quantifying neuronal connectivity and individually for each ROI [50], [51]. In the definition of the *a priori* model of underlying connectivity patterns, we considered six regions of interest including both ipsilesional and contralesional premotor and motor areas. Other areas importantly involved in motor network (*i.e.* cerebellum, prefrontal areas) were excluded from the analysis as in DCM models including more than 8 ROIs, additional prior constraints are needed to reduce the number of parameters to estimate [62]. Moreover, DCM analysis does not result in erroneous estimations when regions that may have an influence on the model are disregarded, because information by brain regions not explicitly modelled is captured implicitly in the coupling parameters between two regions [63].

## *fMRI activation and effective connectivity during a NF-MI task*

Group level fMRI results yield activations of the areas typically involved during a NF MI task: SMA, PMC and posterior parietal cortex (PPC) [64]. These results are also in line with findings indicating that PPC is generally active when feedback is presented visually [65]. Activation patterns evolved from the first session to the last of the training. The first session involved SMA and the last session showed a larger recruitment of bilateral PMC and also a localized activation of ipsilesional M1. The activation of bilateral SMA and ipsilesional M1 during the NF task linearly increased across the 14 training runs, indicating that, in average, patients successfully upregulated the targeted cortical areas. When looking at the individual results (see Figure S3), this linear increase is observed in 6 out of 9 patients. However, this type of analysis only reveal significant changes in a linear fashion, and is not able to quantify less gradual, abrupt changes in activation with time. Moreover, caution must be employed in interpreting these results as a direct indicator of the efficacy of the NF training, considered the lack of blinded assessment and the absence of a comparison with a control group.

SMA is robustly activated during MI [66] and has been associated to complex MI tasks, involving a sequence of movements [64]. Whether M1 is consistently activated during a MI task is debated. Functional MRI NF studies found non-conclusive results at group level [41], [42] and one recent work reported deactivation of M1 during MI training of the SMA and M1 [66]. A recent meta-analysis only reported consistent activation within the primary motor cortex during MI in a minority of studies (18%) [64]. The authors of this study suggest that only skilled MI performer may be able to activate M1 during a MI task, as found for instance by Sharma et al. [67], which could explain why M1 activation can be more consistently reported in single-subject analyses [68]. Our results indicated an activation of ipsilesional M1 in the last NF session suggesting on the one hand that patients “responded” to the NF

reinforcement scheme targeting ipsilesional M1, and on the other that they became better at performing the MI task, which is to be expected after 14 motor NF training sessions.

Average connectivity results are in line with previous studies investigating EC patterns in stroke during MI or execution. They indicate a dense, bilateral connectivity pattern, with an inhibitory connection between contralateral M1 and ipsilesional M1. Connectivity in the contralesional hemisphere is commonly elicited in stroke patients during MI of the affected limb and there is evidence that the inhibitory influence from contralesional M1 to ipsilesional M1 increases in stroke patients with respect to healthy controls [13]. The role of contralesional M1 in stroke is debated as it has been shown to have both promoting and inhibitory influences on motor outcomes, depending on the severity and time from stroke[69]–[71]. For instance, a suppression of the contralesional M1 excitability has been shown to degrade upper limb control in severely impaired patients but to improve it for mildly impaired stroke patients [72].

#### *Effect of NF training on effective connectivity*

Few recent studies have revealed the potential of modulating functional connectivity between the ipsilesional motor cortex and other cortical [34] or subcortical regions [33] for stroke rehabilitation. In a study involving 10 chronic stroke patients, an enhancement of the functional connectivity FC of preserved ipsilesional motor areas with NF led to a significant increase in motor function. This was not the case in a control condition where patients enhanced FC of a brain area not directly implicated in motor function [34]. However, to the best of our knowledge, this is the first work that assesses fMRI connectivity changes resulting from the NF training of target motor areas in stroke. More generally, this work tackles the need to investigate how NF training of localized activity affects the related brain networks to guide more effective NF strategies based on physiologically relevant network targets and to gain a deeper insight into the underlying pathological processes [73].

DCM analysis revealed significant changes in EC after NF training relative to baseline. Firstly, a general decrease in inter-hemispheric connections was observed, including a decrease in the inhibitory influence of the contralesional M1 on the ipsilesional PMC. This inhibitory influence through transcallosal connections reduces the motor output of the damaged hemisphere in patients with severe motor deficit [4], [74], [75], and is part of a well-known “maladaptive” plasticity mechanism in stroke [76]. In a DCM study from Grefkes and colleagues on the effect of transcranial magnetic stimulation applied on contralesional M1, the negative coupling from contralesional M1 was absent as a result of the treatment, and, more interestingly, this effect correlated with improvement in motor performance of the paretic hand [4]. Caution is however recommended when interpreting changes in contralesional M1 connectivity because, even if its alterations in stroke are well-documented, their influence on motor recovery is debated and insufficiently understood [1].

We observed an increase in feedforward connectivity strength between ipsilesional SMA and PMC after the NF training. Using a similar BMA approach, Bajaj and colleagues compared the connectivity before and after mental practice and physical therapy intervention [14]. In line with our findings, they reported an increase in EC between SMA and PMC in the affected hemisphere during MI task and this increase was significantly correlated with the motor score improvement after treatment. Similarly, Sharma and colleagues reported that coupling between PMC and SMA is diminished in stroke patients with respect to healthy controls and that as motor function improved, the coupling between these areas increased [77].

The general reduction of connectivity from ipsilesional to contralesional motor areas (see also Figure S8 in Supplementary Material) suggests a pattern closer to a unilateral motor imagery network in healthy subjects, as the inhibitory influence from M1 to the contralateral motor areas is a well described mechanism of unilateral hand movements [70]. Moreover, an increase in the inhibitory coupling from M1 to SMA and, inversely, a positive coupling from SMA to M1 corresponds to the feed-forward connectivity model estimated with DCM in healthy controls in [78]. More generally, the observed trend of reduction in connectivity can be also interpreted as an effect of learning. Average EC patterns show a fully connected bilateral network during MI (Figure 4A): a decrease in the strength of EC suggests that the same MI task could be performed with a less dense network at the end of the NF training. A similar trend was observed in connectivity patterns during language prosody NF training where connectivity was reduced and more localized at the end of the training [79].

Finally, the decrease in self-inhibitory connections in ipsilesional M1 and bilateral SMA indicates that these regions were more activated at the end of the NF training. As results in Table 2 indicate, the largest change was observed in the ipsilesional M1 (-0.1635), followed by ipsilesional SMA (-0.1339) and contralesional SMA (-0.1195). This is in line with the results of the fMRI activation analysis and, more interestingly, with the NF reinforcement scheme that rewarded upregulation of ipsilesional SMA and M1 that rewarded upregulation of ipsilesional SMA and M1, with a shift towards M1 activation at the end of the training.

#### *Future work*

The population of this study is relatively small and includes stroke patients with a relatively broad range of stroke latency and lesions localization. Individual motor and structural impairment differences following stroke might induce variability to the estimation of EC with DCM. Unfortunately, this is the case of the majority of fMRI-NF studies, whose sample size is strongly limited by the cost and burden of MRI imaging and also true in this case, considered the technical challenge of bimodal EEG-fMRI NF and the fact that patients underwent a long training program of 14 NF sessions over 5 weeks. We designed this experimental protocol with the rationale that NF training induced changes in brain organization would require a significant amount of training. In future, a larger sample of patients will be considered to refine our findings of NF training effect on connectivity networks and extend our observations. For instance in this first study we only examined changes in connectivity at the end of the training protocol. In future work and on a larger cohort we aim to assess if changes in connectivity occur also after a few NF training sessions with finer granularity.

In this exploratory study, we assessed changes in EC estimated from fMRI as it allows for a finer analysis of different motor areas (SMA, PMC and M1) as compared to EEG. In addition, we did not disentangle the role of unimodal EEG and bimodal EEG-fMRI NF in the observed EC changes, as we first assessed if global effect of the NF training on EC could be observed. Future analyses will address these open questions, notably looking at EEG connectivity. Building on these first results, in future work we will also assess if the connectivity changes elicited by NF training resulted in improved motor performance of the affected limb, taking clinical outcomes into account. In order to assess the specific effect of NF training these results needs to be extended with a randomized controlled study, where network reorganization patterns could be compared between the interventional and control group.

Overall, we believe that this work represents a valuable and novel analysis of the large-scale effects of localized NF training on fMRI connectivity, and, to the best of our knowledge, the first in stroke. It



underlines the importance of investigating also connectivity patterns rather than focusing on regional activation when assessing NF training outcomes.

## Conclusions

Using a DCM approach, in this work we investigate the effect of multi-session EEG-fMRI NF training on connectivity patterns in chronic stroke patients. The DCM model consisted in a bilateral motor network including premotor, supplementary and primary motor areas and a Bayesian Model Average approach was used to assess significant changes in connectivity following the NF training. Results show that upregulation of ipsilesional M1 and SMA modulates fMRI activity and effective connectivity in both hemispheres and generally reduces inter-hemispheric connectivity strength. Our results suggest that the upregulation of target motor areas by means of NF can have a larger scale impact on connectivity and a potential to mitigate maladaptive networks patterns.

## Acknowledgements

MRI data acquisition was supported by the Neurinfo MRI research facility from the University of Rennes I. Neurinfo is granted by the the European Union (FEDER), the French State, the Brittany Council, Rennes Metropole, Inria, Inserm and the University Hospital of Rennes. We thank Gabriela Vargas for her useful suggestions for the DCM analysis. The project was supported by the National Research Agency in the “Investing for the Future” program under reference ANR-10-LABX-07-0, and by the “Fondation pour la Recherche Médicale” under the convention #DIC20161236427.

## Author contributions

G.L. wrote the manuscript, A.V. and Q.D. contributed to methods section writing. G.L., I.B., S.B., C.B. and A.L. designed the studies. I.B., S.B. and E.L. contributed to patient enrollment and screening. A.V., G.L., J.C. and Q.D. performed the data analysis. G.L., E.L. and M.F. collected the data. G.L. and E.B. contributed to the design of the experimental platform. All authors reviewed the manuscript.

## References

- [1] A. G. Guggisberg, P. J. Koch, F. C. Hummel, and C. M. Buetefisch, “Brain networks and their relevance for stroke rehabilitation,” *Clin. Neurophysiol.*, vol. 130, no. 7, pp. 1098–1124, 2019.
- [2] H. Johansen-Berg, J. Scholz, and C. J. Stagg, “Relevance of structural brain connectivity to learning and recovery from stroke,” *Front. Syst. Neurosci.*, vol. 4, no. November 2010, 2010.
- [3] A. K. Rehme, S. B. Eickhoff, L. E. Wang, G. R. Fink, and C. Grefkes, “Dynamic causal modeling of cortical activity from the acute to the chronic stage after stroke,” *Neuroimage*, vol. 55, no. 3, pp. 1147–1158, 2011.
- [4] C. Grefkes *et al.*, “Cortical Connectivity after Subcortical Stroke Assessed with Functional Magnetic Resonance Imaging,” *Ann. Neurol.*, vol. 63, pp. 236–246, 2008.
- [5] H. Johansen-Berg, M. F. S. Rushworth, M. D. Bogdanovic, U. Kischka, S. Wimalaratna, and P. M. Matthews, “The role of ipsilateral premotor cortex in hand movement after stroke,” *Proc. Natl. Acad. Sci. U. S. A.*, vol. 99, no. 22, pp. 14518–14523, 2002.

- 525 [6] M. Catani and D. H. Ffytche, "The rises and falls of disconnection syndromes," *Brain*, vol. 128,  
526 no. 10, pp. 2224–2239, 2005.
- 527 [7] W. de Haan, K. Mott, E. C. W. van Straaten, P. Scheltens, and C. J. Stam, "Activity Dependent  
528 Degeneration Explains Hub Vulnerability in Alzheimer's Disease," *PLoS Comput. Biol.*, vol. 8, no.  
529 8, 2012.
- 530 [8] A. Fornito, A. Zalesky, and M. Breakspear, "The connectomics of brain disorders," *Nat. Rev.*  
531 *Neurosci.*, vol. 16, no. 3, pp. 159–172, 2015.
- 532 [9] N. S. Ward, M. M. Brown, A. J. Thompson, and R. S. J. Frackowiak, "Neural correlates of motor  
533 recovery after stroke : a longitudinal fMRI study," vol. 126, no. 0 11, pp. 2476–2496, 2013.
- 534 [10] N. S. Ward, "Future perspectives in functional neuroimaging in stroke recovery," *Eura*  
535 *Medicophys*, vol. 43, pp. 285–294, 2007.
- 536 [11] N. Sharma, J. Baron, and J. B. Rowe, "Motor Imagery After Stroke : Relating Outcome to Motor  
537 Network Connectivity," *Ann. Neurol.*, vol. 66, no. 5, pp. 604–616, 2009.
- 538 [12] A. Lazaridou *et al.*, "fMRI as a molecular imaging procedure for the functional reorganization of  
539 motor systems in chronic stroke," *Mol. Med. Rep.*, vol. 8, no. 3, pp. 775–779, 2013.
- 540 [13] C. Grefkes and G. R. Fink, "Reorganization of cerebral networks after stroke: New insights from  
541 neuroimaging with connectivity approaches," *Brain*, vol. 134, no. 5, pp. 1264–1276, 2011.
- 542 [14] S. Bajaj, A. J. Butler, D. Drake, and M. Dhamala, "Brain effective connectivity during motor-  
543 imagery and execution following stroke and rehabilitation," *NeuroImage Clin.*, vol. 8, pp. 572–  
544 582, 2015.
- 545 [15] K. J. Friston, "Functional and effective connectivity: a review.," *Brain Connect.*, vol. 1, no. 1, pp.  
546 13–36, Jan. 2011.
- 547 [16] L. Wang *et al.*, "Dynamic functional reorganization of the motor execution network after  
548 stroke," *Brain*, vol. 133, no. 4, pp. 1224–1238, 2010.
- 549 [17] F. De Vico Fallani *et al.*, "Evaluation of the brain network organization from EEG signals: A  
550 preliminary evidence in stroke patient," *Anat. Rec.*, vol. 292, no. 12, pp. 2023–2031, 2009.
- 551 [18] L. Wang, J. Zhang, Y. Zhang, R. Yan, H. Liu, and M. Qiu, "Conditional Granger Causality Analysis  
552 of Effective Connectivity during Motor Imagery and Motor Execution in Stroke Patients,"  
553 *Biomed Res. Int.*, vol. 2016, 2016.
- 554 [19] C. Grefkes, D. A. Nowak, L. E. Wang, M. Dafotakis, S. B. Eickhoff, and G. R. Fink, "Modulating  
555 cortical connectivity in stroke patients by rTMS assessed with fMRI and dynamic causal  
556 modeling," *Neuroimage*, vol. 50, no. 1, pp. 233–242, 2010.
- 557 [20] S. M. Smith *et al.*, "Network modelling methods for FMRI," *Neuroimage*, vol. 54, no. 2, pp. 875–  
558 891, 2011.
- 559 [21] M. A. Cervera *et al.*, "Brain-Computer Interfaces for Post-Stroke Motor Rehabilitation: A Meta-  
560 Analysis," *bioRxiv*, pp. 1–22, 2017.
- 561 [22] F. Pichiorri *et al.*, "Sensorimotor rhythm-based brain-computer interface training: The impact  
562 on motor cortical responsiveness," *J. Neural Eng.*, vol. 8, no. 2, 2011.
- 563 [23] T. Wang, D. Mantini, and C. R. Gillebert, "The potential of real-time fMRI neurofeedback for  
564 stroke rehabilitation," *Cortex*, no. S0010-9452(17)30301–5, 2017.
- 565 [24] G. Lioi *et al.*, "A multi-target motor imagery training using bimodal EEG-fMRI Neurofeedback: a

566 pilot study on chronic stroke patients," *Front. Hum. Neurosci.*, vol. 14, no. February, pp. 1–13,  
567 2020.

568 [25] D. E. J. Linden and D. L. Turner, "Real-time functional magnetic resonance imaging  
569 neurofeedback in motor neurorehabilitation," *Curr. Opin. Neurol.*, vol. 29, no. 4, pp. 412–418,  
570 2016.

571 [26] C. Zich, S. Debener, C. Kranczioch, M. G. Bleichner, I. Gutberlet, and M. De Vos, "Real-time EEG  
572 feedback during simultaneous EEG-fMRI identifies the cortical signature of motor imagery,"  
573 *Neuroimage*, vol. 114, pp. 438–447, 2015.

574 [27] E. Bagarinao *et al.*, "Improved volitional recall of motor-imagery-related brain activation  
575 patterns using real-time functional MRI-based neurofeedback," *Front. Hum. Neurosci.*, vol. 12,  
576 no. April, pp. 1–13, 2018.

577 [28] A. Ramos-Murguialday *et al.*, "Brain-Machine-Interface in Chronic Stroke Rehabilitation: A  
578 Controlled Study," *Ann. Neurol.*, vol. 74, no. 1, pp. 100–108, 2014.

579 [29] M. Fleury *et al.*, "A Survey on the Use of Haptic Feedback for Brain-Computer Interfaces and  
580 Neurofeedback," *Front. Hum. Neurosci.*, 2020.

581 [30] C. Jeunet, B. Glize, A. McGonigal, J. M. Batail, and J. A. Micoulaud-Franchi, "Using EEG-based  
582 brain computer interface and neurofeedback targeting sensorimotor rhythms to improve  
583 motor skills: Theoretical background, applications and prospects," *Neurophysiol. Clin.*, 2018.

584 [31] F. Pichiorri *et al.*, "Brain-computer interface boosts motor imagery practice during stroke  
585 recovery," *Ann. Neurol.*, vol. 77, no. 5, pp. 851–865, 2015.

586 [32] C. Zich, "High intensity chronic stroke motor imagery neurofeedback training at home - three  
587 case reports," *Clin. EEG Neurosci.*, 2017.

588 [33] S.-L. Liew *et al.*, "Improving Motor Corticothalamic Communication After Stroke Using Real-  
589 Time fMRI Connectivity-Based Neurofeedback," *Neurorehabil. Neural Repair*, vol. 30, no. 7, pp.  
590 671–675, 2016.

591 [34] A. Mottaz *et al.*, "Modulating functional connectivity after stroke with neurofeedback: Effect on  
592 motor deficits in a controlled cross-over study," *NeuroImage Clin.*, vol. 20, no. July, pp. 336–  
593 346, 2018.

594 [35] R. Sitaram *et al.*, "Acquired control of ventral premotor cortex activity by feedback training: An  
595 exploratory real-time fMRI and TMS study," *Neurorehabil. Neural Repair*, vol. 26, no. 3, pp.  
596 256–265, 2012.

597 [36] K. D. Young, V. Zotev, R. Phillips, M. Misaki, H. Yuan, and W. C. Drevets, "Real-Time fMRI  
598 Neurofeedback Training of Amygdala Activity in Patients with Major Depressive Disorder," *PLoS*  
599 *One*, vol. 9, no. 2, p. e88785, 2014.

600 [37] V. Zotev, R. Phillips, H. Yuan, M. Misaki, and J. Bodurka, "Self-regulation of human brain activity  
601 using simultaneous real-time fMRI and EEG neurofeedback," *Neuroimage*, vol. 85, no. 2014,  
602 pp. 985–995, 2014.

603 [38] L. Perronnet *et al.*, "Learning 2-in-1 : Towards Integrated EEG-fMRI Neurofeedback," *bioRxiv*,  
604 pp. 1–30, 2020.

605 [39] C. M. Stinear, P. A. Barber, M. Petoe, S. Anwar, and W. D. Byblow, "The PREP algorithm predicts  
606 potential for upper limb recovery after stroke," *Brain*, vol. 135, no. 8, pp. 2527–2535, 2012.

607 [40] M. Mano, A. Lécuyer, E. Bannier, L. Perronnet, S. Noorzadeh, and C. Barillot, "How to Build a

608 Hybrid Neurofeedback Platform Combining EEG and fMRI," *Front. Neurosci.*, vol. 11, no. 140,  
609 2017.

610 [41] M. Chiew, S. M. LaConte, and S. J. Graham, "Investigation of fMRI neurofeedback of differential  
611 primary motor cortex activity using kinesthetic motor imagery," *Neuroimage*, vol. 61, no. 1, pp.  
612 21–31, 2012.

613 [42] M. L. Blefari, J. Sulzer, M. C. Hepp-Reymond, S. Kollias, and R. Gassert, "Improvement in  
614 precision grip force control with self-modulation of primary motor cortex during motor  
615 imagery," *Front. Behav. Neurosci.*, vol. 9, no. FEB, pp. 1–11, 2015.

616 [43] R. T. Thibault, A. MacPherson, M. Lifshitz, R. R. Roth, and A. Raz, "Neurofeedback with fMRI: A  
617 critical systematic review," *Neuroimage*, vol. 172, no. December 2017, pp. 786–807, 2018.

618 [44] T. Ros *et al.*, "Consensus on the reporting and experimental design of clinical and cognitive-  
619 behavioural neurofeedback studies (CRED-nf checklist)," *Brain*, vol. 0, pp. 1–12, 2020.

620 [45] S. Heunis, R. Lamerichs, S. Zinger, B. Aldenkamp, and M. Breeuwer, "Quality and denoising in  
621 real-time fMRI neurofeedback : a methods review," *Open Sci. Framew.*, no. June, 2018.

622 [46] J. D. Power, A. Mitra, T. O. Laumann, A. Z. Snyder, B. L. Schlaggar, and S. E. Petersen,  
623 "Comparison of fMRI motion correction software tools," *Neuroimage*, vol. 84, pp. 529–543,  
624 2014.

625 [47] S. Zarrar *et al.*, "The Preprocessed Connectomes Project Quality Assessment Protocol - a  
626 resource for measuring the quality of MRI data.," *Front. Neurosci.*, pp. 2–3, 2015.

627 [48] M. A. Mayka, D. M. Corcos, S. E. Leurgans, and D. E. Vaillancourt, "Three-dimensional locations  
628 and boundaries of motor and premotor cortices as defined by functional brain imaging: A  
629 meta-analysis," *Neuroimage*, vol. 31, no. 4, pp. 1453–1474, 2006.

630 [49] P. Zeidman *et al.*, "A guide to group effective connectivity analysis, part 1: First level analysis  
631 with DCM for fMRI," *Neuroimage*, vol. 200, no. March, pp. 174–190, 2019.

632 [50] K. J. Friston, L. Harrison, and W. Penny, "Dynamic causal modelling," *Neuroimage*, vol. 19, no.  
633 4, pp. 1273–1302, 2003.

634 [51] K. E. Stephan, W. D. Penny, R. J. Moran, H. E. M. den Ouden, J. Daunizeau, and K. J. Friston,  
635 "Ten simple rules for dynamic causal modeling," *Neuroimage*, vol. 49, no. 4, pp. 3099–3109,  
636 2010.

637 [52] K. Friston, J. Mattout, N. Trujillo-Barreto, J. Ashburner, and W. Penny, "Variational free energy  
638 and the Laplace approximation," *Neuroimage*, vol. 34, no. 1, pp. 220–234, 2007.

639 [53] D. Hermes *et al.*, "Functional MRI-based identification of brain areas involved in motor imagery  
640 for implantable brain-computer interfaces," *J. Neural Eng.*, vol. 8, no. 2, 2011.

641 [54] K. J. Friston *et al.*, "Bayesian model reduction and empirical Bayes for group (DCM) studies,"  
642 *Neuroimage*, vol. 128, pp. 413–431, 2016.

643 [55] J. A. Hoeting, D. Madigan, A. E. Raftery, and C. T. Volinsky, "Bayesian Model Averaging: A  
644 Tutorial," *Stat. Sci.*, vol. 14, no. 4, pp. 382–417, 1999.

645 [56] P. Zeidman *et al.*, "A guide to group effective connectivity analysis, part 2: Second level analysis  
646 with PEB," *Neuroimage*, vol. 200, no. May, pp. 12–25, 2019.

647 [57] G. Lioi *et al.*, "Simultaneous MRI-EEG during a motor imagery neurofeedback task: an open  
648 access brain imaging dataset for multi-modal data integration Authors," *bioRxiv*, 2019.

- 649 [58] E. B. Torres, A. Raymer, L. J. G. Rothi, K. M. Heilman, and H. Poizner, "Sensory-spatial  
650 transformations in the left posterior parietal cortex may contribute to reach timing," *J.*  
651 *Neurophysiol.*, vol. 104, no. 5, pp. 2375–2388, 2010.
- 652 [59] K. Mullinger, S. Debener, R. Coxon, and R. Bowtell, "Effects of simultaneous EEG recording on  
653 MRI data quality at 1.5, 3 and 7 tesla," *Int. J. Psychophysiol.*, vol. 67, no. 3, pp. 178–188, 2008.
- 654 [60] T. Hanakawa, M. A. Dimyan, and M. Hallett, "Motor planning, imagery, and execution in the  
655 distributed motor network: A time-course study with functional MRI," *Cereb. Cortex*, vol. 18,  
656 no. 12, pp. 2775–2788, 2008.
- 657 [61] J. F. Smith, K. Chen, A. S. Pillai, B. Horwitz, and A. S. Dick, "Identifying effective connectivity  
658 parameters in simulated fMRI : a direct comparison of switching linear dynamic system ,  
659 stochastic dynamic causal , and multivariate autoregressive models," no. May, pp. 1–17, 2013.
- 660 [62] M. L. Seghier and K. J. Friston, "Network discovery with large DCMs," *Neuroimage*, vol. 68, pp.  
661 181–191, 2013.
- 662 [63] K. Friston, "Dynamic causal modeling and Granger causality Comments on: The identification of  
663 interacting networks in the brain using fMRI: Model selection, causality and deconvolution,"  
664 *Neuroimage*, vol. 58, no. 2, pp. 303–305, 2011.
- 665 [64] S. Héту *et al.*, "The neural network of motor imagery: An ALE meta-analysis," *Neurosci.*  
666 *Biobehav. Rev.*, vol. 37, no. 5, pp. 930–949, 2013.
- 667 [65] R. Sitaram *et al.*, "Closed-loop brain training: The science of neurofeedback," *Nat. Rev.*  
668 *Neurosci.*, vol. 18, no. 2, pp. 86–100, 2017.
- 669 [66] D. M. A. Mehler *et al.*, "The BOLD response in primary motor cortex and supplementary motor  
670 area during kinesthetic motor imagery based graded fMRI neurofeedback," *Neuroimage*, vol.  
671 184, pp. 36–44, 2019.
- 672 [67] N. Sharma, P. S. Jones, T. A. Carpenter, and J. C. Baron, "Mapping the involvement of BA 4a and  
673 4p during Motor Imagery," *Neuroimage*, vol. 41, no. 1, pp. 92–99, 2008.
- 674 [68] P. Dechent, K. D. Merboldt, and J. Frahm, "Is the human primary motor cortex involved in  
675 motor imagery?," *Brain Res. Cogn Brain Res*, vol. 19, no. 2, pp. 138–144, 2004.
- 676 [69] C. Gerloff *et al.*, "Multimodal imaging of brain reorganization in motor areas of the  
677 contralesional hemisphere of well recovered patients after capsular stroke," *Brain*, vol. 129, no.  
678 3, pp. 791–808, 2006.
- 679 [70] C. Grefkes, S. B. Eickhoff, D. A. Nowak, M. Dafotakis, and G. R. Fink, "Dynamic intra- and  
680 interhemispheric interactions during unilateral and bilateral hand movements assessed with  
681 fMRI and DCM," *Neuroimage*, vol. 41, no. 4, pp. 1382–1394, 2008.
- 682 [71] D. A. Nowak, C. Grefkes, M. Ameli, and G. R. Fink, "Interhemispheric competition after stroke:  
683 Brain stimulation to enhance recovery of function of the affected hand," *Neurorehabil. Neural*  
684 *Repair*, vol. 23, no. 7, pp. 641–656, 2009.
- 685 [72] L. V Bradnam, C. M. Stinear, and W. D. Byblow, "Ipsilateral motor pathways after stroke :  
686 implications for non-invasive brain stimulation," *Front. Hum. Neurosci.*, vol. 7, no. May, pp. 1–8,  
687 2013.
- 688 [73] D. S. Bassett and A. N. Khambhati, "A network engineering perspective on probing and  
689 perturbing cognition with neurofeedback," *Ann. N. Y. Acad. Sci.*, pp. 1–18, 2017.
- 690 [74] C. Grefkes and G. R. Fink, "Connectivity-based approaches in stroke and recovery of function,"

691 *Lancet Neurol.*, vol. 13, no. 2, pp. 206–216, 2014.

692 [75] F. De Vico Fallani *et al.*, “Multiscale topological properties of functional brain networks during  
693 motor imagery after stroke,” *Neuroimage*, vol. 83, pp. 438–449, 2013.

694 [76] N. Takeuchi and S. I. Izumi, “Maladaptive plasticity for motor recovery after stroke:  
695 Mechanisms and approaches,” *Neural Plast.*, vol. 2012, 2012.

696 [77] N. Sharma, J. C. Baron, and J. B. Rowe, “Motor imagery after stroke: Relating outcome to motor  
697 network connectivity,” *Ann. Neurol.*, vol. 66, no. 5, pp. 604–616, 2009.

698 [78] C. H. Kasess, C. Windischberger, R. Cunnington, R. Lanzenberger, L. Pezawas, and E. Moser,  
699 “The suppressive influence of SMA on M1 in motor imagery revealed by fMRI and dynamic  
700 causal modeling,” *Neuroimage*, vol. 40, no. 2, pp. 828–837, 2008.

701 [79] G. Rota, G. Handjaras, R. Sitaram, N. Birbaumer, and G. Dogil, “Reorganization of functional and  
702 effective connectivity during real-time fMRI-BCI modulation of prosody processing,” *Brain*  
703 *Lang.*, vol. 117, no. 3, pp. 123–132, 2011.

704

705